



**HAL**  
open science

# Harmonic decomposition to describe the nonlinear evolution of Stimulated Brillouin Scattering

Stefan Hüller, Andrei Maximov, Denis Pesme

► **To cite this version:**

Stefan Hüller, Andrei Maximov, Denis Pesme. Harmonic decomposition to describe the nonlinear evolution of Stimulated Brillouin Scattering. 2003. hal-00000506v1

**HAL Id: hal-00000506**

**<https://hal.science/hal-00000506v1>**

Preprint submitted on 18 Jul 2003 (v1), last revised 25 Jul 2003 (v2)

**HAL** is a multi-disciplinary open access archive for the deposit and dissemination of scientific research documents, whether they are published or not. The documents may come from teaching and research institutions in France or abroad, or from public or private research centers.

L'archive ouverte pluridisciplinaire **HAL**, est destinée au dépôt et à la diffusion de documents scientifiques de niveau recherche, publiés ou non, émanant des établissements d'enseignement et de recherche français ou étrangers, des laboratoires publics ou privés.

# Harmonic decomposition to describe the nonlinear evolution of Stimulated Brillouin Scattering

S. Hüller, A. Maximov\*, and D. Pesme

*Centre de Physique Théorique, Ecole Polytechnique,  
CNRS UMR 7644, 91128 Palaiseau Cedex, France*

(Dated: July 19, 2003)

## Abstract

An efficient method to describe the nonlinear evolution of Stimulated Brillouin Scattering in long scale-length plasmas is presented. The method is based on a decomposition of the hydrodynamics variables in long- and short-wavelength components. It makes it possible to describe the self-consistent coupling between the plasma hydrodynamics, Stimulated Brillouin Scattering, and the generation of harmonics of the excited ion acoustic wave (IAW). This description is benchmarked numerically and proves to be reliable even in the case of an undamped ion acoustic wave. The momentum transferred from the electromagnetic waves to the plasma ions is found to induce a plasma flow which modifies the resonant three wave coupling between the IAW and the light waves. A novel picture of SBS arises, in which both IAW harmonics and flow modification reduce the coherence of SBS by inducing local defects in the density and velocity profiles. The spatial domains of Stimulated Brillouin activity are separated by these defects and are consequently uncorrelated, resulting in a broad and structured spectrum of the scattered light and in a temporally chaotic reflectivity.

PACS numbers: 52.38.Bv, 52.35.Mw, 52.38.-r, 42.65.Es

ccsd-00000506 (version 1) : 19 Jul 2003

---

\* Permanent address : Laboratory for Laser Energetics, University of Rochester, 250 East River Road, Rochester NY 14623, USA

The description of parametric instabilities in laser-produced plasmas using simple coupled mode equations for three wave interaction is no longer sufficient whenever the longitudinal plasma waves are driven to large amplitudes. Then the nonlinearities of the longitudinal wave can induce detuning with respect to the three wave resonance. This is one of the reasons usually invoked to explain why these simplified models overestimate the scattering levels of Stimulated Brillouin Scattering (SBS). In this article we concentrate on SBS, which is the process by which the incident laser wave couples to an ion acoustic wave (IAW) to give rise to a scattered transverse wave. The generation of the harmonics due to the IAW fluid-type nonlinearity [1, 2, 3, 4, 5] is already known to be able to reduce significantly the SBS reflectivity when compared with the results involving simply a linearized IAW. However, the previous fluid-type models for SBS in Refs. [1, 2, 3, 4], aimed at taking into account the IAW nonlinearity, were incomplete because they did not properly describe the flow modification [6, 7] caused by the incident transverse wave momentum deposition. All the mentioned models [1, 2, 3, 4, 5] also ignored multi-dimensional effects. On the other hand, kinetic effects associated with particle trapping [8] give also rise to a nonlinear IAW frequency shift and therefore modify the SBS nonlinear behavior.

In the present Letter, we reconsider the effect of the IAW nonlinearities on SBS by accounting properly for the flow modification caused by SBS. We first derive approximate equations describing simultaneously the plasma hydrodynamics (i.e. the long wavelength density and flow profiles), SBS, and the harmonic generation of the excited IAW resulting from fluid-type nonlinearity. Our method consists in decomposing the fluid variables into long and short wavelength components, the latter corresponding to the SBS generated IAW and its harmonics[9]. Our new code, based on this harmonic decomposition method, makes it possible to describe plasmas of spatial sizes of the order of realistic laser produced plasmas (of mm-size, typically), because it does not resolve the IAW  $\mu\text{m}$ -scale. We then continued a step further by checking the capacity of our approach to account for kinetic effects effects by implementing in the IAW propagator a nonlinear frequency shift modeling particle trapping.[8]

The transverse electric field is described by  $E(\mathbf{x}, t) = e^{-i\omega_0 t} (E_+ e^{ik_0 z} + E_- e^{-ik_0 z}) + c.c.$  where  $E_+(\mathbf{x}, t)$  and  $E_-(\mathbf{x}, t)$  are the forward- and backward propagating light field components, respectively, both enveloped in time and space with respect to the light frequency  $\omega_0$  and the wave number  $k_0$ . This wave number is taken for a fixed reference plasma density

$N_{eq}$  which yields, using the critical electron density  $n_c$ ,  $k_0^2 = \omega_0^2(1 - N_{eq}/n_c)/c^2$ . For the plasma density  $n(\mathbf{x}, t)$  and the velocity  $\mathbf{v}(\mathbf{x}, t)$  we use a decomposition separating the long-wavelength components  $N_0(\mathbf{x}, t)$  and  $\mathbf{v}_0(\mathbf{x}, t)$  and the short-wavelength components  $n_p(\mathbf{x}, t)$  and  $\mathbf{v}_p(\mathbf{x}, t)$ , with  $|p| = 1, 2, \dots$ ,

$$n = N_0 + \left( n_1 e^{ik_s z} + n_2 e^{ik_s z} + \dots + c.c. \right),$$

$$\mathbf{v} = \mathbf{v}_0 + \left( \mathbf{v}_1 e^{ik_s z} + \mathbf{v}_2 e^{ik_s z} + \dots + c.c. \right),$$

the first ( $p=0$ ) representing the hydrodynamic evolution, and the terms with  $p > 0$ , the fundamental ion acoustic wave,  $p = 1$ , excited by SBS, and its harmonics,  $p > 1$ . The reference wave number for the IAW is the wavenumber of backscattering,  $k_s = 2k_0$ , for which the ponderomotive force is proportional to  $\propto E_+ E_-^* \exp(i2k_0 z)$ .

We use the paraxial approximation to reduce the wave equation for the total electromagnetic field  $E$  to two ‘‘paraxial’’ equations for  $E_+(\mathbf{x}, t)$  and  $E_-(\mathbf{x}, t)$ ,

$$\mathcal{L}_{\text{par}}(E_+) = -i(\omega_0/cN_{\text{eq}}) [n_1 E_- + (N_0 - N_{\text{eq}})E_+], \quad (1)$$

$$\mathcal{L}_{\text{par}}(E_-) = -i(\omega_0/cN_{\text{eq}}) [n_1^* E_+ + (N_0 - N_{\text{eq}})E_-], \quad (2)$$

with the paraxial operator  $\mathcal{L}_{\text{par}}(E_{\pm}) = [\partial_t + c_{\pm}\partial_z + \nu_t - i(c^2/2\omega_0)\nabla_{\perp}^2]E_{\pm}$ , where  $c_+$  and  $c_-$  stand for the group velocity of the forward/backward propagating light, respectively, with  $c_+ = c^2 k_0/\omega_0 = -c_-$ , and  $\nu_t$  denotes the damping of the transversal waves. The right-hand-side (rhs) source terms in equations (1) and (2) account for (i) resonant 3-wave coupling due to SBS, with the fundamental ion sound wave,  $n_1$ , and for (ii) refraction on long-wavelength density modifications,  $N_0 - N_{eq}$ , causing e.g. self-focusing. In comparison with the full wave equation without decomposition into  $E_{\pm}$ , this model allows a considerably coarser spatial resolution and thus much less numerical expense.

For the long-wavelength hydrodynamic component we use the following set of equations, assuming isothermal conditions, and written in the conservative form on the left-hand side (lhs):

$$\partial_t N_0 + \nabla N_0 \mathbf{v}_0 = (\partial_t n)_{\text{IAW}}, \quad (3)$$

$$\begin{aligned} \partial_t (N_0 \mathbf{v}_0) + \nabla (N_0 \mathbf{v}_0 \mathbf{v}_0) + c_s^2 \nabla N_0 = \\ -N_0 c_s^2 \nabla U_0 + (\partial_t n \mathbf{v})_{\text{IAW}}, \end{aligned} \quad (4)$$

where the rhs source terms,  $(\partial_t n)_{\text{IAW}}$  and  $(\partial_t n \mathbf{v})_{\text{IAW}}$ , describe the momentum transfer into the flow due to the IAW excitation by SBS, with  $(\partial_t n \mathbf{v})_{\text{IAW}} \equiv 2c_s (2\nu_{s1} - \mathbf{v}_0 \cdot \nabla) |n_1|^2 / N_0$ ,

and  $(\partial_t n)_{\text{IAW}} \equiv -2c_s \nabla (|n_1|^2/N_0)$ . The ponderomotive force is given by  $\nabla U_0 = \epsilon_0 \nabla (|E_+|^2 + |E_-|^2)/n_c T_e$ . The equations describing the IAW driven by SBS,  $n_1$ , and its harmonics,  $n_{l>1}$  (using the convention  $n_{-l} = n_l^*$  for the complex conjugate) can be written, in the so-called weak coupling regime, as follows

$$\begin{aligned} & \left[ \partial_t + \nu_{sl} + i\omega_l + (v_{0z} + v_{gl})\partial_z - i(c_s/2lk_s)\nabla_{\perp}^2 \right] n_l = \\ & -i(k_s c_s/2)N_0 \left[ \delta_{l,1} \left( \epsilon_0 E_+ E_-^*/n_c T \right) + 2Q_l/N_0^2 \right] \end{aligned} \quad (5)$$

with  $Q_l = (l/2) \sum n_h n_{l-h}$  for  $h \neq 0$  and  $l \neq h$ , where  $c_s = [(ZT_e + 3T_i)/M_i]^{1/2}$  is the IAW speed (with  $Z$  and  $M_i$  as the ion charge and mass),  $v_{0z}$  the  $z$ -component of the flow  $\mathbf{v}_0$ ;  $v_{gl}$  and  $\omega_l$  denote the group velocity and the ‘‘local’’ frequency of the  $l$ -th IAW harmonic, both accounting for the dispersion due to Debye shielding increasing with the harmonic order. They are given by  $v_{gl} = c_s(1 + l^2 k_s^2 \lambda_D^2)^{-3/2}$  and by  $\omega_l(z) = \omega_s(lk_s c_s) + lk_s v_{0z}(z)$  with the IAW frequency  $\omega_s(k) = kc_s(1 + k^2 \lambda_D^2)^{-1/2}$ . Equations (1)-(5) describe what we call the harmonic decomposition model. They form a closed system describing SBS in a temporally and spatially evolving plasma. They can be shown to conserve momentum [7] at the lowest order in  $1/(k_s \ell_{\parallel})$  and in  $1/(k_s \ell_{\perp})^2$  (with the inhomogeneity length  $\ell_{\parallel} = |\partial_z v_0/v_0|^{-1}$  and  $\ell_{\perp} = |\nabla_{\perp} v_0/v_0|^{-1}$ ).

In the following we emphasize the particular importance (i) of the SBS-induced flow modification, originating from the rhs term of Eq. (3) as well as of the term  $(\partial_t n \mathbf{v})_{\text{IAW}}$  on the rhs of Eq. (4), and (ii) of the IAW harmonic generation described by the coupling terms  $\propto \sum n_h n_{m-h}$  in the rhs of Eq. (5). In order to stress the effect of each mechanism, we neglect for simplicity the IAW damping, (while being aware that the IAW damping coefficient is usually of the order of a few percent of the IAW frequency). Indeed, the SBS-induced flow modification due to momentum transfer, first pointed out by Rose in Ref.[6], cannot be ignored in the regime of absolute instability corresponding to weak IAW damping, because it is just in this regime that the stationary 1D limit of Eqs. (3) and (4) exhibits the most pronounced flow modification. Namely, the generation of the backscattered light gives rise to a transfer of momentum to the bulk plasma in the spatial domain of SBS activity. This momentum transfer results in a decrease  $\Delta v \equiv v_{0,out} - v_{0,in} < 0$  of the flow  $v_0$  in the direction of propagation of the laser, the net flow decrease being given by  $\Delta v \simeq -2R_{\text{SBS}}(2\epsilon_0|E_+|^2/N_{eq}T_e)(1 - N_{eq}/2n_c)$ . Here,  $R_{\text{SBS}}$  denotes the SBS reflectivity corresponding to the considered SBS active region.

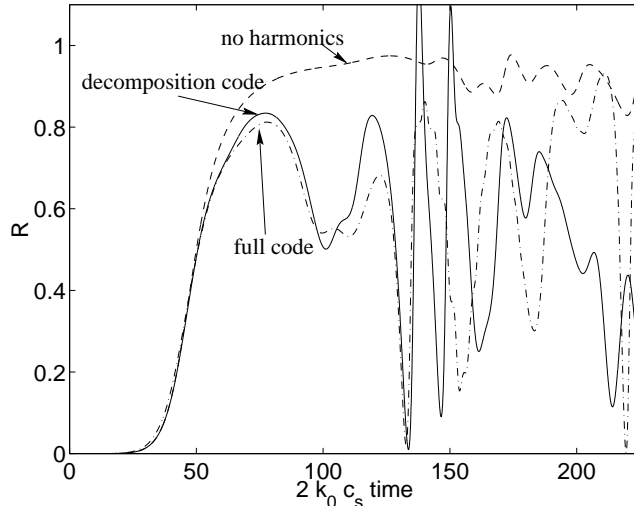


FIG. 1: SBS reflectivity  $R_{\text{SBS}}$  versus time for the case of an undamped IAW with the parameters  $I_L = 2.5 \cdot 10^{14} \text{W/cm}^2$  for  $\lambda_0 = 1.064 \mu\text{m}$  at  $T_e = 1 \text{keV}$ ,  $N_0/n_c = 0.1$  (taken at center),  $2k_0\lambda_D = 0.27$ ,  $L_{\text{ini}} \simeq 160\lambda_0$ . The solid line is obtained from the decomposition code considering all terms, the dashed line from the decomposition code disregarding higher IAW harmonics, and the dash-dotted line from the "full" code.

We have performed simulations on the basis of equations (1)-(5) and expanded the IAW up to its 3rd harmonic, resulting in a set of equations for  $n_1$ ,  $n_2$ , and  $n_3$ , with the rhs terms  $Q_1 = n_2 n_1^* + n_3 n_2^*$ ,  $Q_2 = n_1^2 + 2n_3 n_1^*$ , and  $Q_3 = 3n_2 n_1$ . We did not observe any significant changes when harmonics above the 3rd order were retained, while restricting to less than 3 harmonics led to important differences. At this stage of our study we restricted ourselves to one-dimensional (1D) simulations in order to benchmark our harmonic decomposition code against a "complete" 1D code which does not make the decomposition corresponding to Eqs. (1)-(3). This latter code solves Helmholtz's equation for the total electric field  $E(z, t)$  on the first hand, and the system of fluid equations for continuity and momentum, with the complete ponderomotive force,  $\nabla |E(z, t)|^2$ , as a source term, on the second hand. Here, in 1D, the operator  $\nabla$  reduces to the partial derivative  $\mathbf{e}_z \partial_z$ .

To ensure equivalent boundary and initial conditions we have considered a realistic case similar to an "exploding foil", where an initially heated plasma expands starting from an almost box-like density profile, with smooth shoulders, in the interval  $z_1 < z < z_2$  along the laser axis. The plasma profile, with the initial plateau width  $L_{\text{ini}} \simeq 160\lambda_0$ , successively undergoes rarefaction from each side, so that the velocity profile eventually tends to a

monotonous curve varying from negative to positive values with  $v_0 = 0$  in the center. The simulation box is chosen in such a way that the rarefaction of the profile does not significantly change the boundary conditions for the light fields at the entrance ( $z_{\text{ent}} = 0 < z_1$ ) and the rear side ( $z_{\text{rear}} > z_2$ ). The total box size is  $z_{\text{rear}} = 2000/k_0 \simeq 320\lambda_0$ , where  $\lambda_0 = 2\pi/k_0$  denotes the laser wavelength. The boundary condition for the incident light at  $z = 0$  is a constant,  $E_+(0) = \text{const}$ , whereas the backscattered light is seeded with a noise source at the level  $\langle |E_-(z = z_{\text{rear}})|^2 \rangle \sim 10^{-6}|E_+(z = 0)|^2$  and with a spectral bandwidth sufficiently larger than the IAW frequency, in order to cover all possible SBS resonances in the profile. In the density profile wings left and right of the central plateau (for times  $t < L_{\text{ini}}/2c_s$ ), the plasma is strongly inhomogeneous in velocity and density so that SBS is inhibited by the strong flow gradient.

We carried out our simulations in the absolute instability regime of SBS with undamped IAWs, both to examine the role of flow due to momentum transfer, and to benchmark the robustness of our decomposition code. Notice that in the case of completely undamped IAWs the SBS saturation level is, according to Refs. [10, 11], independent of the noise level. For the chosen electron density  $N_{eq}/n_c = 0.1$  and for the plasma length indicated above, the standard three-wave interaction model for undamped IAWs [10, 11] predicts a steep increase in the SBS reflectivities  $R_{\text{SBS}}$  as a function of the laser intensity, varying from  $R_{\text{SBS}} \ll 1$  for small laser intensities to  $R_{\text{SBS}} \simeq 1$  for normalized laser intensities above  $a_0^2 = \epsilon_0|E_0|^2/n_c T_e \simeq 0.003$ , with  $E_0$  denoting  $E_0 = E_+(z = 0)$ . Our simulations comparing the decomposition code and the “complete” code show very good agreement, even for the extreme case shown in Fig. 1, corresponding to the plasma parameters mentioned above and to  $a_0^2 = 0.025$  and  $2k_0\lambda_D = 0.27$  (corresponding to an electron temperature  $T_e = 1\text{keV}$  and a laser intensity  $I_L = 2.5 \cdot 10^{14}\text{W/cm}^2$  at  $\lambda_0 = 1.064\mu\text{m}$ ), for which the reflectivity would be 99% in the absence of any IAW nonlinearity or flow modifications. For lower intensity values, the agreement is even more striking. This excellent agreement between the two codes gives us confidence in the robustness of the harmonic decomposition description. In the simulation presented in Figs. 1 and 2, the maximum amplitudes of the harmonics remained below the validity condition for harmonic expansion, namely  $|n_l/N_{eq}| < 6^{1/2}(lk_s\lambda_D)^2$  for  $l = 1, 2, 3$ .

It can be observed, in the spatial profiles shown in Fig. 2 for the backscattered intensity  $|E_-|^2$ , the fundamental IAW amplitude  $|n_1|$ , the flow  $v_0$ , and the plasma profile  $N_0$ , that the IAW behavior and flow modifications are entirely connected with the existence of

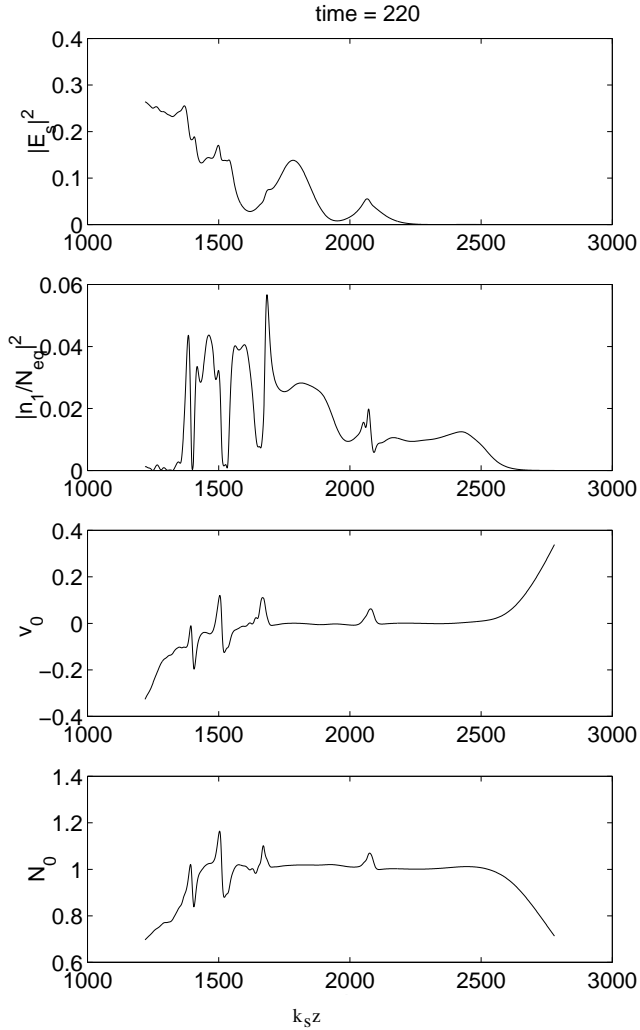


FIG. 2: Spatial profiles, taken at  $2k_0c_s t = 220$ , of the backscattered intensity (upper subplot), the fundamental IAW square amplitude  $|n_1|^2$ , the flow velocity  $v_0$ , and the density  $N_0$  inside the shoulders of the exploding foil profile.

“defects” in these spatial profiles and with a non-monotonous character in space (see also Ref.[4]). Namely, SBS develops in distinct spatial domains, interrupted by phase defects, which originate in the density profile shoulders corresponding to the low density plasma on the laser entrance side, and which then propagate into the profile plateau. Thus the SBS activity in each spatial domain appears to be uncorrelated, due to their different origin in the inhomogeneous velocity profile  $v_0$ . This feature reflects in the structured nature of the backscattered light temporal spectrum, shown in Fig. 3 in which distinct peaks appear, and, consequently, in the temporally chaotic behavior of the reflectivity.



Our decomposition description makes it possible to discriminate the relative importance of the various effects contributing to the nonstationary behavior in the SBS reflectivity, as seen in Fig. 1. By suppressing parts of these effects in different runs, we have found that the most important effect is the excitation of the IAW harmonics: namely, retaining the harmonic excitation and neglecting the SBS-induced flow modification lead to results that remain in reasonably good agreement with the exact model, whereas, retaining the flow modification, but ignoring the harmonics leads to unphysically high levels of IAW amplitudes. It follows from these observations that a realistic modeling of SBS requires the proper description of the IAW harmonics. The 1D simulations presented here would correspond to the SBS development in a long laser hot spot. We have recently carried out 2D simulations which confirm the relevance in 2D of the scenario described above whenever the hot spot focus is not far (less than approximately one Rayleigh length) from the transition between the inhomogeneous and the homogeneous domain of the plasma density profile (i. e. the shoulder of the expanding plasma in our case).

Increasing the laser intensity induces stronger IAW amplitudes at which ion and/or electron kinetic effects take place. We have included phenomenologically weak ion kinetic effects in our decomposition model by adding a non-linear frequency shift of the form  $-i\eta|n_1/N_{eq}|^{1/2}$ , [8] in the propagator appearing in the lhs of Eq. (5) describing the evolution of the IAW fundamental component and of its harmonics. Although this is subject of work in progress, let us mention that we have solved numerically the corresponding equation Eqs. (1)-(5), and we find that for a positive and sufficiently large  $\eta$  coefficient ( $\simeq 0.5 \dots 0.7$ ), this shift can smooth out the effect induced by the harmonics and the flow, in a way such that (i) the “defects” are less pronounced and (ii) the SBS reflectivity diminishes, but without exhibiting a strong nonstationary behavior. In conclusion, we have shown that the SBS modeling presented here, based on a harmonic decomposition of the hydrodynamics variables, represent a promising way to describe laser plasma interaction in long scale-length plasmas. We have benchmarked our code based on the harmonic decomposition in the extreme limit of the absolute instability regime by neglecting the IAW damping. A novel picture of SBS arises in which an incoherent superposition of scattered light generated in distinct spatial domains in the velocity profile leads to a nonstationary character of the SBS reflectivity and to a significant reduction in the time averaged reflectivity. This harmonic decomposition description appears to be sufficiently robust and versatile to allow further sophistication by

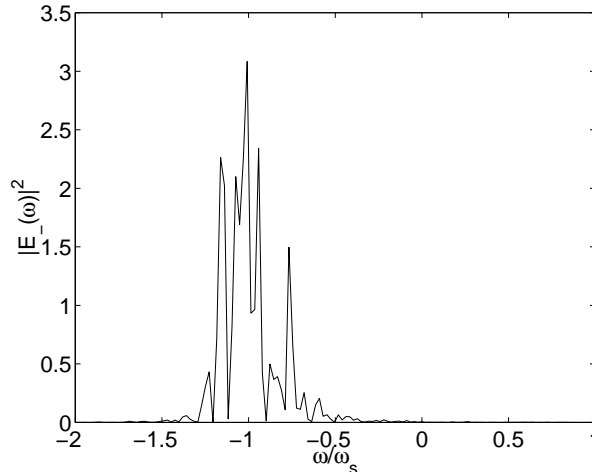


FIG. 3: Spectrum of the backscattered light, corresponding to Fig. 1. The frequency is shifted with respect to the incident laser frequency  $\omega_0$ .

including additional mechanisms such as kinetic effects via an amplitude-dependent nonlinear frequency shift. We currently work on a generalization of the harmonic decomposition method in order to include the subharmonic IAW decay.

The numerical simulation were carried out thanks to the access to the facilities of IDRIS at Orsay, France. The authors would like to acknowledge fruitful discussion with L. Divol, J. Myatt, C. Riconda, H. A. Rose, and W. Rozmus.

- 
- [1] V. P. Silin and V. T. Tikhonchuk, *Sov. Phys. JETP Lett.* **34**, 365 (1981); J. A. Heikkinen, S. J. Karttunen, and R. R. E. Salomaa, *Phys. Lett.* **101A**, 217 (1984); *Phys. Plasmas* **27**, 707 (1984).
  - [2] J. Candy, W. Rozmus, and V. T. Tikhonchuk, *Phys. Rev. Lett.* **65**, 1889 (1990).
  - [3] M. Casanova, G. Laval, R. Pellat, and D. Pesme, *Phys. Rev. Lett.* **54**, 2230 (1985); V. V. Kurin and G. Permittin, *Sov. J. Plasma Phys.* **8**, 207 (1982).
  - [4] W. Rozmus, M. Casanova, D. Pesme, A. Heron, and J.C. Adam, *Phys. Fluids* **B4**, 576 (1992).
  - [5] S. Hüller, *Phys. Fluids* **B 3**, 3317 (1991).
  - [6] H.A. Rose, *Phys. Plasmas* **4**, 437 (1997).
  - [7] D. Pesme et al., *Plasma Phys. Contr. Fusion* **44**, B53 (2002).

- [8] G. J. Morales, and T. M. O'Neil, *Phys. Rev. Lett.* **28**, 417 (1972).
- [9] A similar approach is used in the code F3D, see R. L. Berger, et al., *Phys. Plasmas* **5**, 4337 (1998), but neither IAW harmonics are considered, nor the momentum transfer is described consistently in F3D.
- [10] A. V. Maximov, R. M. Oppitz, W. Rozmus, and V. T. Tikhonchuk, *Phys. Plasmas* **7**, 4227 (2000).
- [11] V. Fuchs, *Phys. Fluids* **19**, 1554 (1976).